

# Dielectric Relaxation Analysis of Biopolymer Poly(3-hydroxybutyrate)

Taha A. Hanafy,<sup>1</sup> Khaled Elbanna,<sup>2</sup> Somyia El-Sayed,<sup>1</sup> Arafa Hassen<sup>1</sup>

<sup>1</sup>Department of Physics, Faculty of Science, Fayoum University, Fayoum 63514, Egypt

<sup>2</sup>Department of Microbiology, Faculty of Agriculture, Fayoum University, Fayoum 63514, Egypt

Received 13 July 2010; accepted 7 December 2010

DOI 10.1002/app.33950

Published online 11 April 2011 in Wiley Online Library (wileyonlinelibrary.com).

**ABSTRACT:** Poly(3-hydroxybutyrate), PHB, is a widely distributed carbon storage polymer among prokaryotes including *Rhizobium*. Capacities of *Rhizobium etli* R13 to produce the bioplastic during growth on media with different carbon sources appeared to be specific carbon-source. In fed batch fermentation, *R. etli* R13 resulted in cell dry weight 6.2 g/L and PHB 51.4%. Gas chromatography-mass spectrometry and gel permeation chromatography analysis revealed that PHB produced from *R. etli* R13 was solely composed of 3-hydroxybutyric acid and the molecular mass of the purified PHB was  $3.4 \times 10^5$  Da with polydispersity 1.47. Dielectric relaxation of PHB has been studied in the temperature and frequency ranges 300–440 K and 10 kHz–4 MHz, respectively. A clear dielectric  $\alpha$  and  $\rho$ -relaxation processes are observed in these

studied ranges of temperature and frequency. The first process is due to the dipole relaxation in the crystalline phase of PHB. The second one is due to the space-charge formation or Maxwell-Wagner-polarization. The  $\alpha$ -relaxation process has been investigated by semiempirical Havriliak-Negami relaxation function. The activation energy ( $E_a$ ) and the relaxation time ( $\tau_0$ ) are calculated using the Arrhenius equation. The dielectric relaxation strength ( $\Delta\epsilon$ ) is strongly temperature dependent. The calculated values of  $E_a$  for ac conductivity,  $\ln(\sigma)$ , of PHB provide information about the presence of electronic conduction. © 2011 Wiley Periodicals, Inc. *J Appl Polym Sci* 121: 3306–3313, 2011

**Key words:** poly(3-hydroxybutyrate); *Rhizobium etli* R13; relaxation processes; conduction mechanism

## INTRODUCTION

Polyhydroxyalkanoates (PHAs) are a sort of biological polyester, which function as carbon and energy reserves in prokaryotic cells; many different bacteria synthesize PHA when a carbon source is provided in excess and one essential growth nutrient is limited.<sup>1–5</sup> These bacterial polyesters have attracted industrial attentions as environmentally nontoxic, biodegradable, and biocompatible thermoplastics to be used for a wide range of industrial, agricultural, and medical applications.<sup>6–8</sup> They have a high degree of polymerization, are highly crystalline, optically active and isotactic, piezoelectric and insoluble in water. These features make them highly competitive with polypropylene, polyethylene and the petrochemical-derived plastics.<sup>9</sup> Poly(3-hydroxybutyrate) (PHB) is a homopolymer of 3-hydroxybutyric acid. X-ray diffraction reveals that the purified polymer has crystallinity ratio of 67% with orthorhombic crystal shape.<sup>10</sup> Differential scanning calorimetry (DSC) showed a melting enthalpy ( $\Delta H_m$ ) of 62.31 J/g and melting temperature ( $T_m$ ) of 448 K.

The glass rubber transition temperature ( $T_g$ ) is  $\sim 285$ – $291$  K, while thermal degradation occurs around 523 K.

Relaxation properties are very important in polymer processing. Many processes are characterized as being elastic, while others as viscous. Relaxation properties can be studied by dynamic mechanical spectroscopy (DMS), dielectric relaxation spectroscopy (DRS), or nuclear magnetic resonance (NMR) spectroscopy. Relaxation processes play a dominant role and in a complex pattern of temperature and frequency-dependent properties.<sup>11</sup> DRS is a useful method to investigate structure property relationships of polymers. This method is sensitive to molecular fluctuation of dipoles within the system. These fluctuations are related to the molecular mobility of groups, segments or wholly polymer chains which show up as different relaxation processes. The relaxation time ( $\tau_0$ ) of these processes was found to depend on the molecular shape and the molecular friction forces encountered by the rotating dipoles. Moreover, the dipole motions within the amorphous and crystalline phases have a big effect on the semi-crystalline polymer.<sup>12,13</sup> Structural transitions in polymers are generally accompanied by changes in the relaxation properties. When an oscillatory electric field is applied to a polymeric material, several types of polarization are operative: electronic, ionic,

Correspondence to: T. A. Hanafy (tahanafy2@yahoo.com).

orientational, or space charge. A dielectric spectrum is a complicated manifestation of the combination of these operative polarization sources. Orientational and space charge polarization are particularly important when structural transitions are concerned. For polymers, many relaxation modes are involved in orientational polarization. They can be grouped into local processes, cooperative processes in longer chain sequences, chain diffusion, and specific processes in semicrystalline states.<sup>14</sup>

Reported DRS studies on PHB and its blends are scarce. DRS was used to investigate the influence of semicrystalline morphology on the molecular mobility of the crystallized PHBs<sup>15,16</sup> and its blend with polyvinyl acetate PVAc.<sup>17,18</sup> The presence of the crystallinity had a significant effect on the  $\alpha$ -relaxation characteristics of the various cold-crystallized PHBs when compared with the wholly amorphous material. The dielectric spectrum of the previous blends was resolved into three processes  $\alpha$ ,  $\alpha'$ -relaxation processes and ionic conductivity based on Havriliak-Negami and ionic conductivity equations. The Maxwell-Wagner-Sillars (MWS) interfacial polarization effect (i.e.,  $\rho$ -relaxation process) can also be seen in the dielectric permittivity curve of semicrystalline polymer such as polyvinyl alcohol PVA.<sup>19,20</sup> This work is aimed to study the production of PHB by *Rhizobium etli* R13 to explore the dielectric relaxation properties of PHB over a wide range of temperature and frequency. Comparison to previous results and similar materials will be discussed.

## SAMPLE PREPARATION AND EXPERIMENTAL DETAILS

### Microorganism and production of biomass containing PHB

The microorganism used in the present study was *Rhizobium etli* R13 (accession number FJ263092).<sup>21</sup> To evaluate the production of PHB from different carbon sources by *R. etli* R13, batch fermentations were carried out in 250 mL Erlenmeyer flasks containing 100 mL of sterile YEM broth.<sup>22</sup> To optimize production of PHB from *R. etli* R13, fed batch fermentation (80 h) were performed using YEM broth containing 1% mannitol. The flasks were inoculated with 4% of freshly grown preculture and incubated at 30°C on a rotary shaker at 150 rpm and 2% glucose was added after 48 h. At regular intervals, the samples were taken (as whole flasks in duplicate) and centrifuged at 5000 rpm for 30 min at 4°C and washed twice with saline solution, then lyophilized for further analysis. For polymer isolation, lyophilized cells were resuspended in 250 mL of chloroform for 3 days, and then filtered through filter paper. PHB extract was concentrated and precipitated with

diethyl ether. The precipitate was redissolved in chloroform and the process was repeated twice to obtain pure PHB.

### Polymer samples preparation for GC and GC/MS analysis

Lyophilized cells (5–10 mg) were suspended in 1.0 mL chloroform and subjected to methanolysis in 1 mL methanol in the presence of 15% (v/v) sulfuric acid. The methanolysis was performed for 3–5 h at 100°C in an oil bath, and then 1 mL water was added to the cooled mixture and mixed thoroughly for 30 s. After phase separation, the resulting methyl esters of the corresponding fatty acids constituent were assayed by gas chromatography (GC). Gel permeation chromatography (GPC) was used to estimate the molecular weight of the purified PHB. Therefore, GPC system (model 410, Waters Corp, Milford) was used. The purified polymer was dissolved in chloroform (5–10 mg/mL) and subjected to GPC system; applying four sequentially arranged Styragel HR3-6 columns for separation and a model 410 differential refractometer for detection. Polystyrene standards dissolved in chloroform (0.1% w/v) were employed to construct the calibration curve.

### Preparation of PHB films and dielectric spectroscopy measurements

Poly(3-hydroxybutyrate) film was obtained by dissolving the polymer in chloroform at temperature 30°C with continuous stirring. The aqueous solution was cast into a Petridish, placed on a leveled plate at room temperature for 5 days until the solvent was completely evaporated. The obtained PHB film, 0.1 mm thickness, was cut into square pieces and coated with silver paste to achieve ohmic contacts. Dielectric spectroscopy measurements were accomplished using a Hioki (Ueda, Nagano, Japan) model 3532 High Tester LCR, with the accuracy of order  $\pm 0.08\%$ . The dielectric constant ( $\epsilon'$ ), and dielectric loss ( $\epsilon''$ ) were recorded at frequency and temperature ranging from 10 kHz to 4 MHz and from 300 to 440 K, respectively. Both dielectric constant,  $\epsilon'$ , and dielectric losses,  $\epsilon''$ , were calculated as follows:

$$\epsilon' = \frac{Cd}{\epsilon_0 A} \quad \text{and} \quad \epsilon'' = \epsilon' \tan \delta \quad (1)$$

where  $C$  is the capacitance of the sample filled capacitor,  $d$  is the sample thickness,  $\epsilon_0$  is the vacuum permittivity, and  $A$  is the electrode area. The temperature was measured with a T-type thermocouple with its junction just in contact with the sample with accuracy better than  $\pm 1$  K.

## RESULTS AND DISCUSSION

Poly(3-hydroxybutyrate) is a widely distributed carbon storage polymer among prokaryotes including *Rhizobium*.<sup>23</sup> It was found that capacities of *R. etli* R13 to produce the bioplastic during growth on media with different carbon sources appeared to be specific carbon-source. Five different carbon sources such mannitol, glucose, sucrose, fructose and lactose were evaluated for production of high cell density and PHB accumulation. Among these substrates mannitol appears to be the most suitable for biomass production (5 g/L) followed by glucose (4 g/L), sucrose (3.2 g/L), fructose (3.0 g/L) and lactose (2.7 g/L). Whereas, glucose was the most favorable substrate for PHB accumulation (46%) followed by sucrose (42.2%), fructose (34.6%) and lactose (33.5%). To optimize bacterial growth and production of PHB, fed batch fermentation was performed. The cell dry mass and PHB percentage of *R. etli* R13 during the time course of 80 h were presented in Figure 1. As seen, the maximum biomass was 6.2 g/L and the maximum PHB accumulation was 51.4% per cell dry weight.

Many nitrogen-fixing microorganisms synthesize PHB. According to Tombolini and Nuti,<sup>24</sup> the content of this polymer in rhizobia ranges from 30 to 55% of dry cell weight. It was found that PHB synthesis can be selectively induced either in active or less active *Rhizobium* strains by sources of carbon and nitrogen<sup>25</sup>. Because chemical structure and molecular mass are important factors to determine the physical properties of polymers, the purified polymer was analyzed using gas chromatography-mass spectrometry (GC/MS) and GPC. Figure 2 represents GC/MS spectrum of methyl ester 3HB. The produced PHB by *Rhizobium etli* R28 was solely composed of 3-hydroxybutyric acid. In addition, GPC

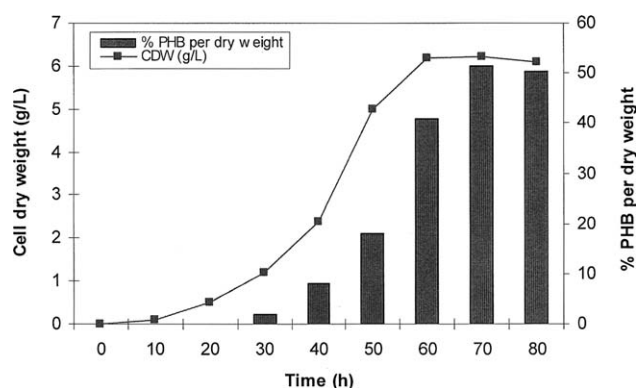


**Figure 1** PHB yield and cell dry weight of *R. etli* during the fed batch fermentation. *R. etli* grown on YEM broth supplemented with 1% mannitol at the beginning of fermentation. After 48 h, glucose was added with 0.5% (w/v) until the final concentration reached 2% (w/v).

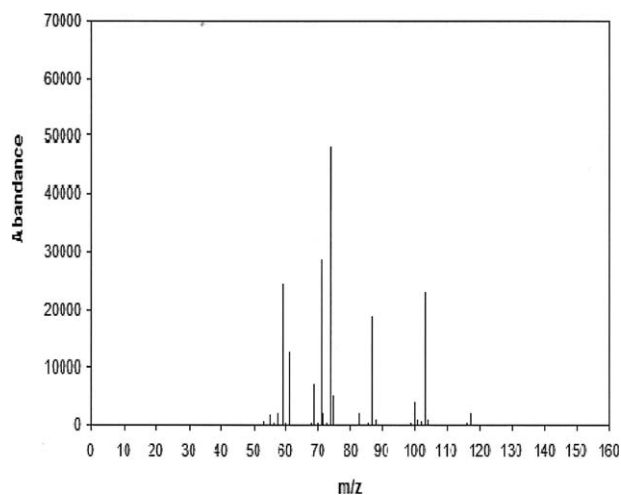


**Figure 2** GC/MS spectrum of 3HB-methyl ester indicating that the PHB produced by *Rhizobium etli* R28 was solely composed of 3-hydroxybutyric acid.

analysis showed that the molecular mass of the purified PHB was  $3.4 \times 10^5$  Da with polydispersity 1.47.

The temperature dependence of  $\epsilon''$  of PHB at selected frequencies is shown in Figure 3. A broad relaxation peak in  $\epsilon''$  was observed at 370 K. This peak becomes narrow and moves towards the low temperatures as the frequency increases. Such behavior can be attributed to the space charge polarization (i.e., the  $\rho$ -relaxation process). This effect occurs at temperature higher than  $T_g$  (285–291 K)<sup>10</sup> and at a low field frequency. The nature of  $\rho$ -relaxation process seems to vary depending on the polymeric material. For semicrystalline polymer, chain trapping at interfaces inside the sample or Maxwell-Wagner polarization (MWS) phenomena is expected.

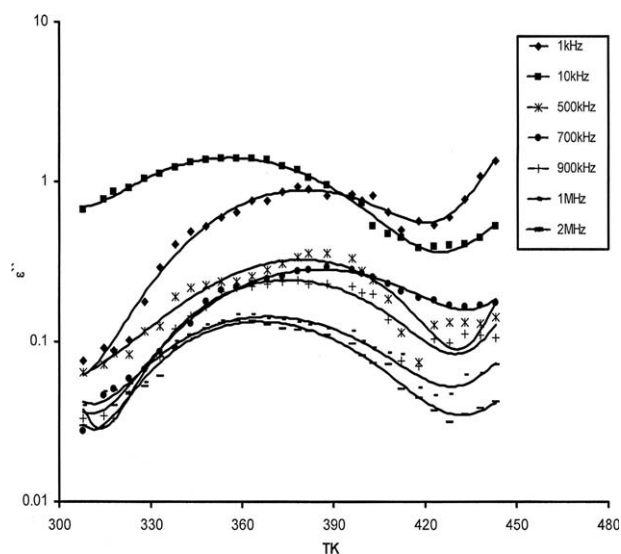


**Figure 3** The temperature dependence of  $\epsilon''$  for PHB at some selected frequencies.

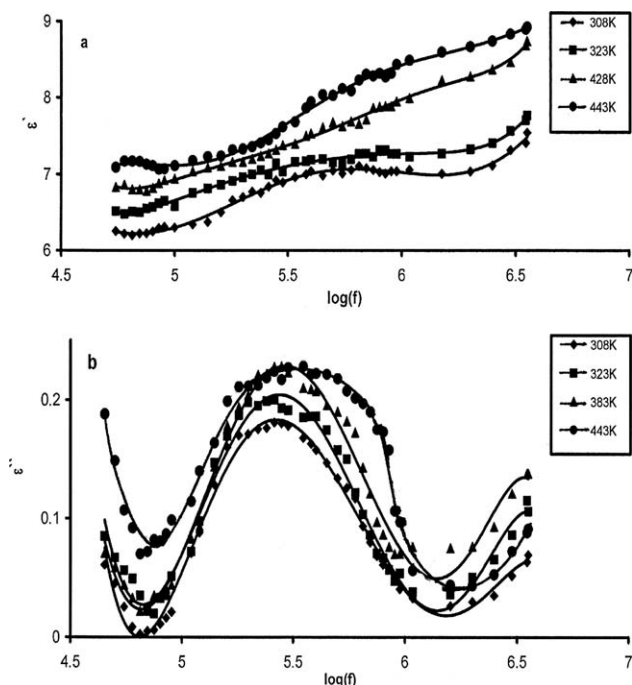


**Figure 4** Frequency dependence of: (a)  $\epsilon'$  and (b)  $\epsilon''$  of PHB at some selected temperatures.

For an amorphous materials,  $\rho$ -relaxation process may be attributed to cooperative parameters such as impurities, injected space charges and electrode effects.<sup>20</sup>

The isothermal plots for  $\epsilon'$  and  $\epsilon''$  versus frequency at selective fixed temperatures are presented in Figure 4(a,b). The dielectric constant,  $\epsilon'$ , increases smoothly with increasing temperature and frequency. This can be attributed to the increase of the thermal energy, which is absorbed by the dipoles of PHB. Consequently, the dipoles have sufficient energy to orientate themselves easily in the direction of the applied field. On the other hand, the increase in  $\epsilon'$  with temperature is assigned to the disentanglement of the molecular chains which becomes easier due to molecular vibrations.<sup>26</sup> The dependence of  $\epsilon'$  on temperature reflects the orientational distribution of the polymer chains in the crystalline as well as in the amorphous regions inside the sample.<sup>16,27</sup> In other words, the number of the polar C=O and methyl, CH<sub>3</sub>, groups become free to rotate with increasing applied field and temperature. From Figure 4(b), one can observe that  $\epsilon''$  of PHB undergoes a single relaxation peak at 316 kHz in the studied frequency range due to  $\alpha$ -relaxation process. The peak position of  $\alpha$ -process shifts to higher frequencies with increasing temperatures and it can be characterized as a dipolar relaxation.

The origin of the  $\alpha$ -transition has been attributed to several mechanisms, such as a rotation of crystalline sequence followed by a translation along the

chain axis, torsional twisting in crystalline sequence, fold movements, or even point defect mechanisms.<sup>28</sup> The crystallinity ratio of PHB has a significant effect on the  $\alpha$ -relaxation characteristics of various cold-crystallized samples when compared with the wholly amorphous materials. The constraining influences of the crystallites produce a progressive relaxation broadening and a positive offset in relaxation temperature.<sup>16</sup> Also, all cold-crystallized PHB/PVAc blends exhibit two glass-rubber ( $\alpha$  and  $\alpha'$ ) relaxations according to the coexisting of mixed amorphous interlamellar phase, and a pure PVAc phase residing in interfibrillar regions.<sup>18</sup> The  $\alpha'$ -relaxation process is related to the rigid amorphous phase located between adjacent lamellar inside the lamellar stacks.<sup>29–33</sup> The  $\alpha'$ -relaxation process was observed in the PHB blends with 30 wt % of PVAc.<sup>17</sup> So,  $\alpha$ -relaxation process of PHB can be assigned to the segmental motion in the crystalline phases within the sample. By other words this process is probably due to the dipole relaxation inside the lamellar stacks.

The dielectric dispersion of the aliphatic polyester as a function of frequency in the vicinity of  $T_g$  relaxation can be described by Havriliak-Negami (HN) phenomenological equation.<sup>34–37</sup> Then, the complex dielectric permittivity  $\epsilon^*$  is given by:

$$\epsilon^* = \epsilon_\infty + \frac{\Delta\epsilon}{[1 + (i\omega\tau_0)^\beta]^\gamma} \quad (2)$$

where  $\Delta\epsilon = \epsilon_s - \epsilon_\infty$ , is the dielectric strength,  $\epsilon_s$  and  $\epsilon_\infty$  are the relaxed and unrelaxed dielectric constants, respectively.  $\tau_0$  is the relaxation time,  $\beta$  and  $\gamma$  are the shape parameters that describe the symmetric and asymmetric broadening of  $\tau_0$ , respectively.

The study of the dielectric behavior of PHB by Cole-Cole plot ( $\epsilon''$  vs.  $\epsilon'$ ) provides valuable information about the dielectric relaxation process. Cole-Cole equation is given by<sup>38</sup>:

$$\epsilon^* = \epsilon_\infty + \frac{\Delta\epsilon}{1 + (i\omega\tau_0)^{1-\gamma}} \quad (3)$$

where  $\tau_0$  is the mean relaxation time and  $\gamma$  is the distribution parameter that ranges from 0 to 1. So, Figure 5 shows the Cole-Cole representation at different fixed temperatures, where data points ( $\epsilon''$  vs.  $\epsilon'$ ) form an arc when a dielectric relaxation occurs in the examined frequency interval. The values  $\tau_0$  and  $\gamma$  have been evaluated using the equation<sup>39</sup>:

$$\frac{U}{V} = (\omega\tau_0)^{1-\gamma} \quad (4)$$

where  $U$  is the distance from a particular data point in the Cole-Cole plot from point  $\epsilon_\infty$  and  $V$  is the distance of the same data point from point  $\epsilon_s$ .

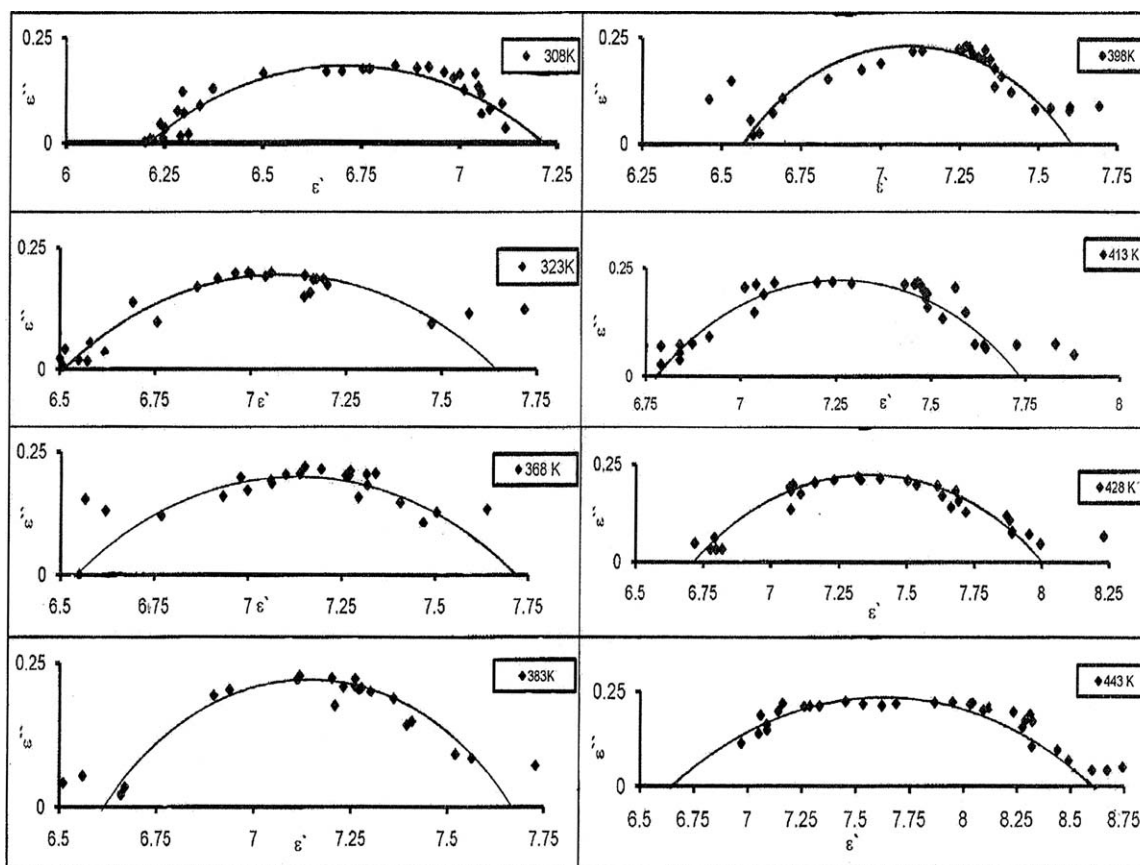


Figure 5 Argand plots at some selected temperatures for PHB.

The calculated values of  $\gamma$  and  $\tau_0$ , are tabulated in Table I. The Arrhenius law for  $\alpha$ -relaxation process is:

$$\tau_0(T) = A \exp\left(\frac{E_a}{kT}\right) \quad (5)$$

where  $E_a$  is the activation energy,  $k$  is Boltzmann constant, and  $A$  is a pre-exponential factor. Figure 6(a) depicts the relaxation time ( $\tau_0$ ) as a function of the inverse of the temperature as calculated from the Cole-Cole curves. The calculated value of  $E_a$  was

found to be of  $\approx 0.3$  eV. Figure 4(b) shows that the maximum frequency,  $f_{\max}$ , of the  $\epsilon''$  peak as a function of the inverse temperature.  $f_{\max}$  was described by the equation:

$$f_{\max} = f_0 \exp\left(\frac{-E_a}{kT}\right) \quad (6)$$

where  $f_0$  is constant. The calculated value of  $E_a$ , according to eqs. (5) and (6), of  $\alpha$ -relaxation process is 0.3 eV. This value is lower than that of the earlier

TABLE I  
The Calculated Values of the Distribution Parameter ( $\gamma$ ) and the Average Relaxation Time ( $\tau_0$ ) According to Cole-Cole Plots of PHB

| T (K) | $\gamma$ | $\tau_0$ (s)          |
|-------|----------|-----------------------|
| 308   | 0.877    | $7.70 \times 10^{-4}$ |
| 323   | 0.766    | $3.22 \times 10^{-4}$ |
| 338   | 0.866    | $3.01 \times 10^{-4}$ |
| 353   | 0.855    | $1.69 \times 10^{-5}$ |
| 368   | 0.833    | $1.06 \times 10^{-4}$ |
| 383   | 0.833    | $6.77 \times 10^{-5}$ |
| 398   | 0.888    | $6.61 \times 10^{-5}$ |
| 413   | 0.833    | $6.19 \times 10^{-5}$ |
| 428   | 0.900    | $6.63 \times 10^{-5}$ |
| 443   | 0.877    | $4.56 \times 10^{-5}$ |

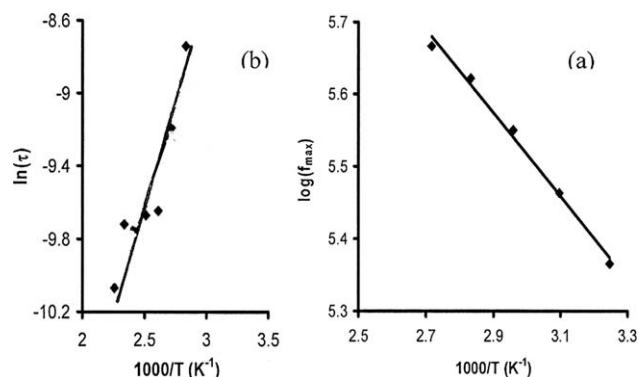
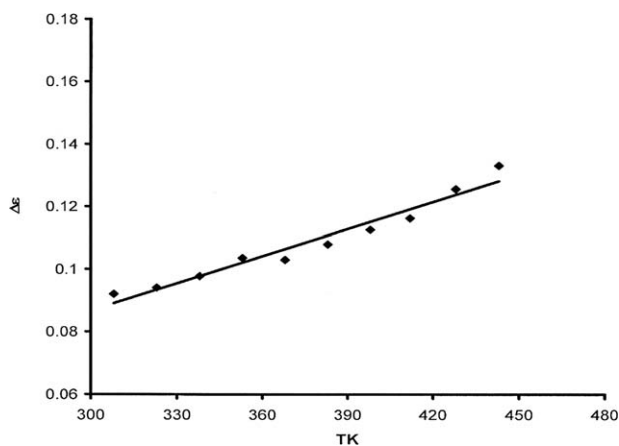


Figure 6 (a) Arrhenius plot of the logarithm of  $f_{\max}$  versus  $1000/T$  for PHB. (b) Arrhenius plot of  $\ln(\tau)$  against  $1000/T$  for PHB.



**Figure 7** The temperature dependence of the dielectric relaxation strength ( $\Delta\epsilon$ ) for PHB.

report (1.0 eV).<sup>40</sup> The low value of  $E_a$  of  $\alpha$ -relaxation process could be explained by the lower bulkiness of the  $\text{CH}_3$  and  $\text{C}=\text{O}$  groups within the amorphous and the crystalline phases of PHB. A similar behavior has been reported for polyethylene terephthalate (PET).<sup>11</sup> Consequently, the low value of  $E_a$  of PET compared with those obtained for poly ethylene naphthalate (PEN) was assigned to the lower bulkiness of the terephthalate ring compared to the more bulky naphthalate group in PEN.<sup>11</sup>

The temperature dependence of dielectric strength,  $\Delta\epsilon$ , of PHB obtained from the above analysis is displayed in Figure 7. It is clear that the values of  $\Delta\epsilon$  increase with the increase of the temperature. This can be attributed to the cooperation exists between thermal energy and the electric field effects of the dipole alignments. Increasing the thermal energy of  $\text{CH}_3$  and  $\text{C}=\text{O}$  groups will tend to enhance the alignment of themselves with the direction of the applied electric field and therefore  $\Delta\epsilon$  increases. It has been reported for the amorphous PHB that  $\Delta\epsilon$  is decreased with increasing temperature due to the decrease of the volume fraction of the mobile amorphous region in the PHB/PVAc blends.<sup>11</sup> However, the increase of  $\Delta\epsilon$  with temperature for the crystalline PHB and PHB/PVAc blends were interpreted to the existence of a rigid amorphous phase which relaxes gradually above the  $T_g$  of the mobile amorphous material.<sup>10</sup> When the crystalline ratio of pure PHB increases up to 67%, an increase of  $\Delta\epsilon$  is expected.

To suppress the electrode effect, the complex electric modulus  $M^*$  is used to explore and analyze the dielectric spectra. The electric modulus  $M^*$  has the following form<sup>40,41</sup>:

$$M^* = \frac{1}{\epsilon^*} = M' + iM'' \quad (7)$$

$$M'(\omega) = \frac{\epsilon'(\omega)}{\epsilon'(\omega)^2 + \epsilon''(\omega)^2} \quad (8)$$

$$M''(\omega) = \frac{\epsilon''(\omega)}{\epsilon'(\omega)^2 + \epsilon''(\omega)^2} \quad (9)$$

Figure 8 shows  $M''(T)$  spectra obtained by transforming the data of Figure 3(b) to  $M^*$  formalism [eq. (8)]. It is observed that PHB undergoes  $\rho$ -relaxation process, which shifts to lower temperature with increasing frequencies. Also, the peak values of  $M''$  were found to be lower than the values of  $\epsilon''$  that obtained from Figure 3(b). This indicates the removal of the electrode polarization. It is also interesting to note that  $\rho$ -relaxation process becomes evident only when the temperatures are higher than  $T_g$  (285–291 K). At temperature higher than 370 K, a growth in  $M''$  with decreasing field frequency is observed. Dc conduction alone will not affect the behavior of  $M''$ . Another relaxation process must have something to do with the mobilization of space charges. It is assigned to MWS interfacial polarization process which originates from the created charges by contact of different phases of different charge conductivity. It can be suggested that the intrinsic relaxation spectra of PHB samples are characterized by a combination of an MWS process and dc conductivity effect. In addition, the charge carriers which are trapped by the surrounding crystallites, accumulate at the interface and move through the amorphous phase under the influence of an applied field. The mobility of these charge carriers should also increase with the increase of the temperature so that the relaxation time becomes shorter. The bulk conductivity in amorphous samples is closely related to ion mobility. The behavior of the trapped charge carriers should resemble those of the global charge carriers which are responsible for bulk conductivity.

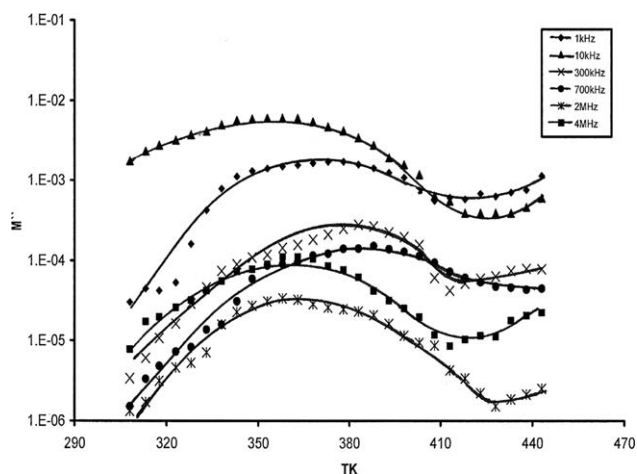


**Figure 8** The variation of the dielectric modulus  $M''$  as a function of temperature at some fixed frequencies for PHB.

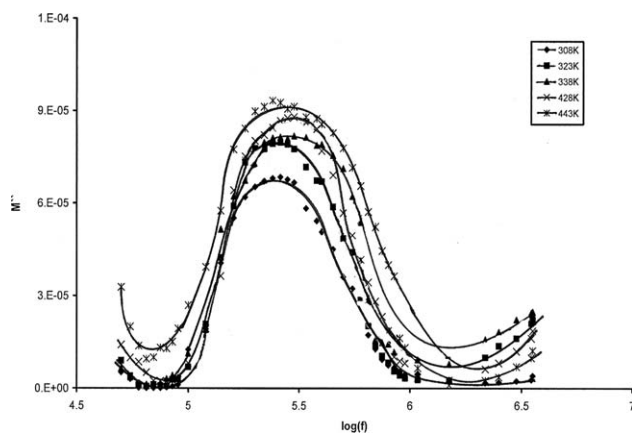


**Figure 9** Variation of the dielectric modulus  $M''$  as a function of frequency at some fixed temperatures for PHB.

The frequency dependence of  $M''$  is represented in Figure 9. At  $f = 316$  kHz,  $\alpha$ -relaxation process of PHB is observed and shifted to higher frequencies with increasing temperature. This peak contributes to the conductivity as seen in Figure 4(b). The shifts of the maximum  $M''$  with temperature corresponds to the conductivity current relaxation. At each temperature, the region to the left of the conductivity current relaxation peak (low frequency side) extends to a long distance since the charge carriers are mobile. On the other hand, the conductivity current relaxation peak (high frequency side) does not move to contribute to the conduction process because the charge carriers are spatially confined to their potential wells.

The temperature dependence of ac conductivity  $\ln(\sigma)$  of PHB is shown in Figure 10. Within the studied range of temperature,  $\ln(\sigma)$  exhibits two straight regions; I at (303–357 K) and II at (400–454 K). The

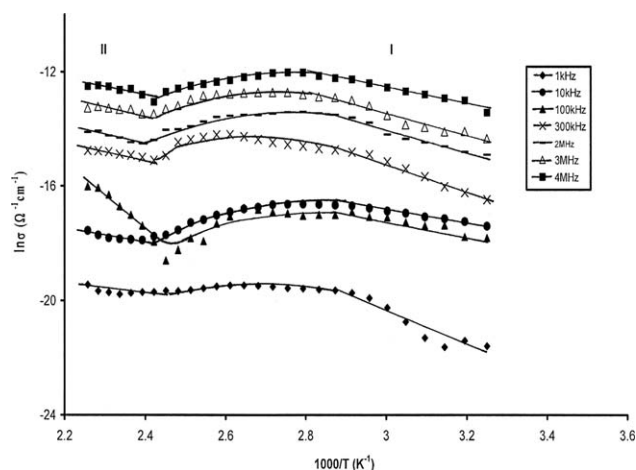


**Figure 10** The temperature dependence of the ac conductivity,  $\ln(\sigma)$ , for PHB at some selected frequencies.

**TABLE II**  
The Calculated Values of the Activation Energy ( $E$ )  
Based on the ac Conductivity of PHB

| $f$ (kHz) | $E$ (I) (eV) | $E$ (II) (eV) |
|-----------|--------------|---------------|
| 1         | 0.76         | 0.30          |
| 10        | 0.20         | 0.30          |
| 100       | 0.23         | 0.86          |
| 300       | 0.45         | 0.45          |
| 500       | 0.45         | 0.45          |
| 700       | 0.45         | 0.14          |
| 900       | 0.45         | 0.23          |
| 2000      | 0.27         | 0.22          |
| 3000      | 0.31         | 0.20          |
| 4000      | 0.27         | 0.20          |

behavior of  $\ln(\sigma)$  within these two regions can be described according to the Arrhenius equation:

$$\sigma = \sigma_0 \exp\left(-\frac{E}{kT}\right) \quad (10)$$

where  $\sigma_0$  is constant, and  $E$  is the activation energy. The  $E$  values were calculated for PHB sample at different frequencies and listed in Table II. It is clear that the values of  $\ln\sigma$  in both regions (I and II) were found to increase with the increase of the field frequency. This may be due to the increase of the absorbed energy which leads to increase the number of the charge carriers that contribute to the conduction process. Moreover, this reveals that the conduction mechanism could be a hopping one.<sup>42,43</sup> Also, the variation of the conductance with temperature is due to a combined effect of a change in the conductance with temperature and the nature of the trap distribution inside the matrix of PHB. It might indicate that the conductance takes place via hopping of carriers between randomly distributed trapping centers in amorphous and crystalline phases. From Table II, one can recognize that the values of  $E$  vary from 0.22 to 0.45 eV. Therefore, the conduction mechanism is mainly electronic and partially ionic as a result of bulk conduction with the different phases that exist in PHB.

## CONCLUSIONS

GC/MS and GPC analysis revealed that PHB produced from *R. etli* R13 was solely composed of 3-hydroxybutyric acid and PHB has a high molecular weight to be used in different industrial applications. The dielectric behavior of PHB undergoes two relaxation processes namely  $\alpha$  and  $\rho$ . The first one is attributed to the dipole relaxation inside the crystalline regions. The second one is the space-charge transition which is due to the chain trapping at the interfaces or MWS polarization within PHB. The dielectric strength  $\Delta\epsilon$  of PHB was strongly

temperature dependent. The Cole-Cole exponent  $\gamma$  shows that there is a distribution in the relaxation times for PHB. The mean relaxation time  $\tau_0$  and  $f_{\max}$  of  $\alpha$ -relaxation process verify Arrhenius type dependence. The behavior of ac conductivity indicates that, the conduction mechanism of PHB could be hopping one.

The authors would like to sincerely thank Prof. Dr. A. Steinbüchel (Westfälische Wilhelms Universität, Münster, Germany) for GC/MS analysis.

## References

- Shen, X. W.; Yang, Y.; Jian, J.; Wu, Q.; Chen, G. Q. *Bioresour Technol* 2009, 100, 4296.
- Cavalheiro, J. M. B. T.; Catarina, M.; de Almeida, M. D.; Grandfils, C.; da Fonseca, M. M. R. *Process Biochem* 2009, 44, 509.
- Sheu, D.-S.; Chen, W. M.; Yang, Y., Jr.; Chang, R.-C. *Enzyme Microb Technol* 2009, 44, 289.
- Papageoriou, A. C.; Wan, S. H.; Singh, C. B.; Jendrossek, D. *J Mol Biol* 2008, 382, 1184.
- WuLiu, X.; Wang, H. H.; Chen, J. Y.; Taoli, X.; Chen, G. Q. *Biochem Eng J* 2009, 43, 72.
- Steinbüchel, A. In *Biomaterials*; Byrom, D., Ed.; MacMillan: London, England, 1991; pp 123–213.
- Lee, S. Y. *Biotechnol Bioeng* 1996, 49, 1.
- Trivedi, T. U.; Patel, K. *Ind. J Biotech* 2006, 5, 137.
- Reddy, C. S. K.; Ghai, R.; Rashmi, V. C. *Bioresour Technol* 2003, 87, 137.
- Pal, S.; Paul, A. K. *Curr Sci* 2002, 83, 1565.
- Becker, O.; Simon, G. P.; Rieckmann, T.; Forsythe, J.; Rosu, R.; Volker, S.; Shea, M. O. *Polymer* 2001, 42, 1921.
- Nouh, S. *Radiat Meas* 2004, 38, 167.
- Mahrous, S. *Int J Polym Mater* 2004, 53, 1.
- Strobl, G. *The Physics of Polymer*, 2nd ed.; Springer-Verlag: New York, 1997.
- Daly, J. H.; Hayward, D.; Liggat, J. J.; Mackintosh, A. R. *J Mater Sci* 2004, 39, 925.
- Shafee, E. E. *Eur Polym J* 2001, 37, 1677.
- Madbouly, S. A.; Mansour, A. A.; Abdou, N. Y. *Eur Polym J* 2007, 43, 3933.
- Shafee, E. E. *Eur Polym J* 2001, 37, 451.
- Boyd, R. H.; Liu, F. In *Dielectric Spectroscopy of Polymeric Materials*; Runt, J. P., Fitzgerald, J. J., Eds.; American Chemical Society: Washinton, DC, 1997.
- Hanafy, T. A. *J Appl Polym Sci* 2008, 108, 2540.
- Elbanna, K.; Elbadry, M.; Gamal-Eldin, H. *Syst Appl Microbiol* 2009, 32, 522.
- Vincent, J. M. *A Manual for the Practical Study of Root Nodule Bacteria*, 1st ed.; Black Well Publishers: Oxford, 1970; p164.
- Jha, P. K.; Nair, S; Babu, C. R. *J Basic Microbiol* 1993, 33, 389.
- Tombolini, R.; Nuti, M. D. *FEMS Microbiol* 1989, 60, 299.
- Bonartseva, G. A.; Myshkina, V. L.; Zagreba, E. D. *Microbiology* 1994, 63, 45.
- Flory, P. J. *Principles of Polymer Chemistry*; Cornell University Press Ithaca: New York, 1953.
- Brown, S. B.; Orlando, C. M. In *Encyclopedia of Polymer Science and Engineering*; Wiley-Interscience; John Wiley & Sons: New York, 1988.
- Laredo, E.; Suarez, N.; Bello, A.; Bello, A.; Marquez, L. *J Polym Sci Part B: Polym Phys* 1996, 34, 641.
- Alie, J.; Menegotto, J.; Cardon, P.; Caron, H. A.; Lacabanne, C. *J Pharm Sci* 2004, 93, 218.
- Wurm, A.; Soliman, R.; Schick, C. *Polymer* 2003, 44, 7467.
- Wurm, A.; Soliman, R.; Goossens, J. G. P.; Bras, W.; Schick, C. *J Non-Cryst Solids* 2005, 351, 2773.
- den Berg, O. V.; Sengers, W. G. F.; Jager, W. F.; Picken, S. J.; Wubbenhorst, M. *Macromolecules* 2004, 37, 2460.
- Napolitano, S.; Wubbenhorst, M. *Macromolecules* 2006, 39, 5967.
- Turky, G.; Shaaban, S. S.; Schoenhals, A. *J Appl Polym Sci* 2009, 113, 2477.
- Sen, S.; Boyd, R. H. *Eur Polym J* 2008, 44, 3280.
- Mansour, S. H.; Abd-El-Messieh, S. L.; Abd-El-Nour, K. N. *J Appl Polym Sci* 2008, 109, 2258.
- Spall, S.; Good Win, A. A.; Zipper, M. D.; Simon, G. P. *J Polym Sci Part B: Polym Phys* 1996, 34, 2419.
- Singh, N. K.; Kumar, P.; Roy, O. P.; Rai, R. *J Alloy Comp* 2010, 507, 542.
- Prajati, A. N.; Rana, V. A.; Vyas, A. D. *J Mol Liq* 2009, 144, 1.
- Mahrous, S. *Polym Int* 1996, 40, 261.
- Jonscher, A. K. *Dielectric Relaxation in Solids*; Chelsea Dielectric: London, 1983.
- Suzhu, Y.; Hing, P.; Xiao, H. *J Appl Phys* 2000, 88, 398.
- Hanafy, T. A. *Curr Appl Phys* 2008, 8, 527.